Published in final edited form as:
Ann Neurol. 2011 July ; 70(1): 22–29. doi:10.1002/ana.22472.

Evolution of the Blood-Brain Barrier in Newly Forming Multiple Sclerosis Lesions

María I Gaitán, MD[1], **Colin D Shea**[1], **Iordanis E Evangelou Dphil**[1], **Roger D Stone**[1], **Kaylan M Fenton**[1], **Bibiana Bielekova, MD**[1], **Luca Massacesi, MD**[1,2], and **Daniel S Reich, MD, PhD**[1,3]

[1]Neuroimmunology Branch, National Institute of Neurological Disorders and Stroke, National Institutes of Health, Bethesda, MD 20892, USA

[2]Department of Neurological and Psychiatric Sciences, University of Florence, Florence, Italy

Abstract

Objective.—Multiple-sclerosis (MS) lesions develop around small, inflamed veins. New lesions enhance with gadolinium on magnetic resonance imaging (MRI), reflecting disruption of the blood-brain barrier (BBB). Single time point results from pathology and standard MRI cannot capture the spatiotemporal expansion of lesions. We investigated the development and expansion of new MS lesions, focusing on the dynamics of BBB permeability.

Methods.—We performed dynamic-contrast-enhanced (DCE) MRI in relapsing-remitting MS. We obtained data over 65 minutes, during and after gadolinium injection. We labeled spatiotemporal enhancement dynamics as *centrifugal* when initially central enhancement expanded outward and *centripetal* when initially peripheral enhancement gradually filled the center.

Results.—We detected thirty-four enhancing lesions in 200 DCE-MRI scans. In 65%, enhancement first appeared as a closed ring; in 18%, as a nodule; and in 18%, as an open ring. Lesions with initially nodular enhancement were smaller than those initially enhancing as rings ($p<0.0001$). All initially nodular lesions enhanced centrifugally, whereas initially ringlike lesions enhanced centripetally, becoming nodular if small (82%) or nearly nodular if larger (18%). Open-ring lesions were periventricular or juxtacortical and enhanced centripetally. Centrifugally enhancing lesions evolved into centripetally enhancing lesions over several days.

Interpretation.—The rapid change of enhancement dynamics from centrifugal to centripetal reflects the outward growth of MS lesions around their central vein and suggests that factors mediating lesion growth and tissue repair derive from different locations at different times. We propose a model of new lesion growth that unites our imaging observations with existing pathology data.

Introduction

MS is an inflammatory demyelinating disease of the central nervous system. As Charcot described in 1868[1] and as shown by MRI more recently[2], a small vein centers the MS plaque. Many studies (but not all) suggest that the pathogenic processes involved in the onset and enlargement of MS plaques start from lympho-monocytic infiltrates surrounding that vein[3, 4]. There is also perivascular inflammation around small blood vessels at the edges of expanding lesions and in the normal-appearing white matter (NAWM)[3, 5].

[3]Corresponding author: 10 Center Drive MSC 1400, Building 10 Room 5C103, Bethesda, MD 20892, USA. (301) 496-1801, reichds@ninds.nih.gov.

MRI with intravenous injection of gadolinium, a contrast agent that shortens the longitudinal (T_1) relaxation time, detects BBB disruption in new MS lesions[6-9]. BBB opening is usually associated with new lesions and consequently with immune infiltration originating in the area surrounding parenchymal microvessels[10]. *In vitro* and *in vivo*, soluble mediators such as cytokines and chemokines can destabilize the BBB[10-12]. Blood-brain barrier opening in the absence of perivascular inflammatory cuffs is also found near histologically active MS lesions[8, 13, 14].

According to their pattern of contrast enhancement on static MRI, lesions have been classified as nodular or ringlike[15-17]. Ringlike lesions are reportedly associated with more severe tissue damage[15, 16], and open-ring lesions, in particular, are described as characteristic of demyelinating diseases[18]. However, there are no clear histologic differences between ringlike and nodular lesions[6], so some have postulated that distinct enhancement patterns may merely be a consequence of the timing of image acquisition after gadolinium administration[19]. Alternatively, these patterns may represent different immune responses across individuals or different lesion types (i.e., nodular lesions may be newly forming whereas ringlike lesions may be re-enhancing)[20, 21]. What remains unclear in newly forming, enhancing lesions, is whether gadolinium leaks from the opened central vein, from secondarily opened vessels throughout the lesion, or from small blood vessels with or without perivascular inflammation in the surrounding NAWM[5, 22].

DCE-MRI, in which T_1-weighted images are rapidly acquired during and after gadolinium injection, has been used to estimate hemodynamic parameters in MS lesions[23, 24]. This technique can also elucidate the spatiotemporal dynamics of lesion enhancement[25], which may in turn help clarify mechanisms of lesion development and expansion, dynamics of BBB permeability, and the association between static and dynamic enhancement patterns.

Methods

Participants.

We scanned consecutive participants with RRMS (Table 1) under an IRB-approved natural-history protocol. Within 6 months of the scan period and unaware of the MRI findings, an experienced clinician determined disability according to the Expanded Disability Status Scale (EDSS)[26].

MRI protocol.

We performed DCE-MRI (Table 2) on 1.5 and 3.0 tesla (T) MRI scanners (Signa Excite HDxt, GE, Waukesha, WI) using an 8-channel receive-only coil array (Invivo, Gainesville, FL). We acquired whole-brain sagittal 3D Fast Spoiled Gradient Recalled Echo (FSPGR) images during and after a 60sec intravenous infusion of gadolinium-DTPA (Magnevist, Bayer, Leverkusen, Germany) via power injector (MEDRAD, Warrendale, PA) at a standard dose of 0.1mmol/kg. During and after infusion, we acquired 8 consecutive T_1-weighted volumes (total time=4.6min). We collected 2-3 delayed sets of scans, each comprising 2-8 whole-brain volumes, within 30min at 1.5T and 65min at 3.0T.

We also collected higher resolution T_1-weighted images before and after gadolinium as well as T_2-weighted Fluid Attenuation Inversion Recovery (FLAIR) images after gadolinium. Based on the identification of new lesions, we re-scanned 4 participants 5-14 days after their initial scan with high-resolution DCE-MRI. We dedicated these scans to follow-up imaging of newly forming lesions (Table 2).

Image post-processing.

We analyzed all MRI data using MIPAV (http://mipav.cit.nih.gov) and JIST (http://nitrc.org/projects/jist). Using the Optimized Automatic Registration plug-in, we rigidly coregistered all dynamic volumes to the first scan in which arterial enhancement was evident, interpolating to 1mm isotropic resolution. We subsequently transformed all images, again with rigid registration, to Montreal Neurological Institute standard space.

We first identified enhancing lesions >5mm in diameter on the static T_1-weigthed post-gadolinium scans. We then determined the initial enhancement pattern of these lesions according to their appearance on the first dynamic T_1-weighted volume in which we clearly discerned enhancement, as follows: *nodular* (homogeneous hyperintensity throughout the lesion); *closed ring* (complete peripheral hyperintense rim surrounding a hypointense center); and *open ring* (incomplete hyperintense rim with a semi-lunar configuration). We determined the dynamic enhancement pattern from the 4D time series to be *centrifugal* (enhancing from the center to the periphery) or *centripetal* (enhancing from the periphery to the center).

Statistical analysis.

We performed statistical analyses using Stata 9.0 (StataCorp, College Station, TX). We report results as mean ± standard deviation and conducted all statistical tests without adjustment for multiple comparisons. We used two-sample t-tests and one-way analyses of variance to determine whether disease duration or age differed according to the presence or size of enhancement. We used chi-squared tests to analyze whether sex or treatment status was related to the presence or size of enhancement and Wilcoxon's rank-sum test to compare EDSS scores. For comparison of lesion size, initial and dynamic enhancement patterns, and time of data acquisition, we used multilevel mixed-effects linear regression models to account for the possibility of multiple enhancing lesions per participant or multiple scans of the same lesion.

Results

Participants.

We studied 80 people with RRMS, acquiring 200 MRI scans over an 8-month period. We classified participants according to findings on high-resolution post-gadolinium T_1-weighted scans, as follows: group A, at least one contrast-enhancing lesion >5mm in diameter; group B, at least one enhancing lesion <5mm on any scan but no enhancing lesions >5mm; and group C, no enhancing lesions on any scan (Table 1). As expected, people with enhancing lesions had shorter estimated disease duration (years elapsed since first MS symptoms; p=0.01) and were less likely to be taking disease-modifying therapy (p=0.008).

Initial enhancement pattern.

In high-resolution T_1-weighted scans obtained 5-35min after gadolinium injection, we found 34 new enhancing lesions >5mm in diameter. Examination of the dynamic scans showed that in 22 (65%), enhancement was initially closed-ring; in 6 (18%), nodular; and in 6 (18%), open-ring (Table 3). Initially nodular lesions were smaller (5.8±1.2mm) than initially ringlike lesions (p<0.0001), regardless of whether the rings were closed (9.6±4.4mm; p=0.03) or open (12.8±4.1mm; p<0.0001). There was no significant size difference between closed- and open-ring lesions.

Enhancement dynamics.

All initially ringlike lesions enhanced centripetally. In the first few dynamic scans, we observed a fine, uniform ring of enhancement, followed by centripetal thickening of the ring. The entire lesion eventually filled, effectively resulting in nodular enhancement, in 82% of cases (Fig. 1b-c; Supplementary Video 1, 2B). A small central area remained unenhanced in the other 18% (Supplementary Video 3). Of initially ringlike lesions, those that remained ringlike at the end of the study were larger (14.8±5.4mm) than those that became completely nodular (8.2±2.8mm; $p<0.001$). There was no significant difference in the duration of post-gadolinium dynamic scanning comparing lesions that remained ringlike (43±15min) to those that completely filled (36±18min).

All initially nodular lesions enhanced centrifugally. A small, central area of enhancement expanded progressively over several minutes into a larger nodule (Fig. 1a; Supplementary Video 2A). Lesions that enhanced centrifugally were smaller (5.8±1.2mm; $p<0.0001$) than those that enhanced centripetally (10.3±4.4mm). Note that we excluded lesions <5mm in diameter from the analysis because the image resolution was too low to accurately assess the enhancement dynamics. Since the centrifugally enhancing lesions we characterized were smaller, it is possible that by excluding small lesions we underestimated the true proportion of centrifugally enhancing lesions.

Five days after the initial scan, we acquired additional images of a centrifugally enhancing lesion, using dedicated dynamic MRI at higher resolution, and found that the lesion had enlarged and now enhanced centripetally. Twenty-five days later, the enhancement dynamics were persistently centripetal (Fig. 1A-C; Supplementary Video 2A-B). We investigated the dynamic change in signal intensity over time in central and peripheral regions of interest. In the center, the slope and relative amount of enhancement became progressively shallower and lower as the lesion aged, whereas in the periphery they became steeper and higher (Fig. 1G-H).

In 3 additional participants, we also obtained high-resolution follow-up imaging of lesions that were initially <5mm in diameter (too small to be included in the current study) or had unclear enhancement patterns on dynamic scans. On those follow-up scans, which were performed within 2 weeks of the initial scan, 2 of the lesions had enlarged and enhanced centripetally, and the third was no longer enhancing. Centripetally enhancing lesions never became centrifugally enhancing.

All 6 open-ring lesions enhanced centripetally. As with initially closed-ring lesions, the enhancing rim in open-ring lesions was at first thin and eventually became broader. None of the open-ring lesions completely filled in over time. All were located in the periventricular or juxtacortical white matter, and the open portion of the ring faced either the ventricle or the cortex (Fig. 2).

Discussion

Brain MRI has enormous value for detecting and characterizing MS lesions. In particular, the introduction of gadolinium-enhanced scanning demonstrated the important role of BBB permeability in the development of new lesions[8, 27, 28]. The number and volume of such lesions are frequent outcome measures in treatment trials[29, 30]. However, most MRI studies have ignored dynamic aspects of lesion enhancement, which makes it difficult to elucidate the mechanisms and pathology behind the observed lesion enhancement patterns.

Our examination of the enhancement dynamics of new MS lesions reveals that initially nodular lesions enhance centrifugally and are significantly smaller than initially ringlike

lesions. On the other hand, initially ringlike lesions enhance centripetally and later fill in, completely in most cases and partially when the lesions were larger. Thus, previous characterizations of lesion enhancement pattern (ringlike or nodular) were no doubt confounded by both lesion size and time of scanning relative to gadolinium injection.

We also observed that centrifugally enhancing lesions and very small lesions can expand over the course of days and change their enhancement dynamics to centripetal, but we never observed the opposite. This process may reflect the typical way in which MS lesions grow, which would suggest that different static enhancement patterns (ringlike and nodular) actually represent different stages of a single pathogenic process rather than distinct lesion types. Thus, we suggest that enhancing lesions are best characterized either by their initial appearance on post-gadolinium scans, when the enhancement is very faint, or – more accurately – by their dynamic enhancement pattern. Such a characterization would provide relatively specific information about a lesion's age and, by reference to the pathology literature, some insight into its histological features.

More broadly, the MRI data presented here have implications for understanding the biology of lesion development in MS. Specifically, at the time of scanning, the enhancement dynamics reflect vascular permeability to small molecules in the setting of an appropriate concentration gradient between plasma and the extracellular space within the lesion. Since gadolinium fills the lesion but fails to penetrate the surrounding normal tissue, the enhancement dynamics also reflect the relative ease of diffusion within the lesion. On the other hand, the MRI data do not directly report on whether soluble factors such as cytokines, chemokines, and vasoactive peptides pass into and through lesions in the same manner as gadolinium chelates, nor do they elucidate the roles of such factors in the development and/or repair of new MS lesions. Nevertheless, taken together the data imply the following: (1) that lesions grow outward from the central vein; and (2) that in the setting appropriate concentration gradients, gadolinium is more likely to diffuse into a lesion, where the normal tissue architecture is damaged, than into the surrounding healthy tissue.

Our data are summarized schematically in Figure 3, which depicts the transit of gadolinium chelates (and, by inference, whichever endogenous factors behave similarly to those chelates) during MS lesion development. The model emphasizes the opening and closing of the BBB of different vessels within the lesion at different times. Initially (Figure 3A), the BBB opens in and around the central vein[12], a process that may be the downstream result of antigen-specific immune-cell activation in the perivascular space. At this stage, peripheral vessels that are within and just beyond the border of the still expanding lesion are not yet open. Demyelination and tissue damage then spread radially from the central vein, a process that is mirrored in the centrifugal enhancement dynamics that we observed (Fig. 3B).

As the lesion expands, the BBB of peripheral veins and capillaries opens, both within and just outside the area of demyelination [10, 11]. This is consistent with observations that in the vicinity of active lesions, vessels can leak serum proteins, a process that can occur even in the absence of inflammatory cell infiltration [8, 13, 31]. At this stage, the enhancement pattern changes from centrifugal to centripetal (Fig. 3C). The concomitant reduction in central enhancement may be due to closing or partial closing of the BBB of the central vein and contiguous vessels. Another possibility, which may occur in parallel with the first, is a reduction in perfusion of the lesion core [32], with the result that less gadolinium reaches the center than the periphery. Indeed, redirection of blood flow to the lesion periphery must be present when a great number of peripheral vessels are open, which must be the case since peripheral enhancement occurs nearly simultaneously even in portions of the lesion that may be centimeters apart.

The final stage of the model is the termination of lesion growth (Fig. 3D). There are two probable mechanisms for this, again not mutually exclusive. The first is that the final lesion size is determined by the quantity, quality, and duration of the initial immune activation that leads to release and diffusion of soluble inflammatory factors. In this scenario, the termination of lesion growth is a passive process, characterized by exhaustion of pathogenic factors with subsequent spontaneous tissue repair. The second possibility is that the termination of lesion growth represents an active process, perhaps triggered by the secondarily opened BBB and mediated by different immune mechanisms (e.g., immune regulatory cells) or by the response of brain tissue to the original injury (mediated, for example, by microglia and astrocytes)[33]. In this case, lesion growth stops when the balance between pathogenic and repair factors reaches equilibrium. Previous work has demonstrated that the location of the intensely enhancing rim, at its maximal extent, may be beyond the edge of the MRI-visible lesion that remains once enhancement resolves [25, 34] . This finding suggests that an open BBB does not necessarily portend long-term tissue damage and supports the possibility that at the edge of MS lesions, enhancement may reflect a response to tissue damage.

Our model, based on dynamic imaging evidence *in vivo*, is consistent with the pathology literature. To our mind, especially important among prior observations is Adams's description in 1975[3] of the onset and expansion of new MS lesions, starting with lympho-monocytic perivenular infiltrates. Also highly relevant is the detailed description of newly forming lesions provided by Henderson et al. in 2009[5]. This study demonstrated that expanding lesions have three concentric areas surrounding an antigen-specific, adaptive immune reaction: (1) a central region, heavily demyelinated and filled with macrophages containing myelin degradation products; (2) an intermediate region, partly demyelinated and infiltrated by myelin-containing macrophages; and (3) a peripheral region, with intact myelin, activated microglia, and some oligodendrocyte loss.

The failure of juxtacortical lesions to form a complete ring may be related to the fact that the BBB remains closed in cortical lesions, even in actively demyelinating ones[35], perhaps due to differences in microglial activation between gray and white matter[36]. Since the enhancement dynamics of open-ring and closed-ring lesions are the same, we conjecture that these two types of lesion evolve by similar mechanisms, expanding from a perivenular nidus in the white matter. In the case of open-ring lesions, when the expanding lesion reaches the gray-white junction, it meets structural or physiologic barriers that prevent disruption of the cortical BBB and limit the extent of gadolinium diffusion into the cortex. Periventricular lesions have open-ring configurations because the ventricle itself limits their radial expansion.

Limitations and future work.

The principal limitation of this study is that our scans were not of sufficient spatial resolution to determine the dynamic enhancement pattern in lesions <5mm in diameter, a problem that will require dedicated, high-resolution studies. An additional important limitation of the results presented here is the lack of data about tissue characteristics in the months prior to the onset of enhancement. Given previous observations[32, 37, 38] of abnormal diffusion, perfusion, and magnetization transfer characteristics in pre-lesional white matter, it would be interesting to know whether these abnormalities are present throughout the future lesion or focally around the central vein. A third limitation is the lack of histopathology data to test our model, a problem that may be addressed in studies of enhancement dynamics in animal models.

It would also be interesting to observe enhancement dynamics in other brain diseases. Quantitative modeling of tissue permeability, based on DCE-MRI, has been extensively

performed in tumors, but qualitative reports of enhancement dynamics are sparse[39, 40]. If the typical centripetal pattern of enhancement is specific for demyelinating lesions, including tumefactive ones, the results of this study may provide a powerful tool in clinical practice to identify and distinguish demyelinating lesions.

Conclusion

DCE-MRI provides a unique window into the real-time, *in vivo* physiology of new MS lesions. Our findings require replacement of the previously accepted discrimination of nodular and ringlike lesions based on single post-gadolinium T_1-weighted scans in favor of a paradigm based on spatiotemporal enhancement dynamics. Further, they suggest that lesion expansion is rapid and follows a common pattern, possibly based on centrifugal spread of soluble factors and the ability of the immune system and/or endogenous brain cells to respond to the injury they induce.

Supplementary Material

Refer to Web version on PubMed Central for supplementary material.

Acknowledgments

The Intramural Research Program of the National Institute of Neurological Disorders and Stroke supported this work. We thank the study participants, the Neuroimmunology Branch clinical group for evaluating participants and coordinating the scanning, and the NIH Functional Magnetic Resonance Imaging Facility technologists for acquiring much of the data. We also thank Drs. H. McFarland and I. Cortese for critically reviewing the manuscript and providing helpful suggestions.

References

1. Charcot JM. Histologie de la sclérose en plaques. Gaz des Hôp (Paris). 1868; 41:554–66.
2. Tan IL, van Schijndel RA, Pouwels PJ, et al. MR venography of multiple sclerosis. AJNR Am J Neuroradiol. Jun-Jul; 2000 21(6):1039–42. [PubMed: 10871010]
3. Adams CW. The onset and progression of the lesion in multiple sclerosis. J Neurol Sci. Jun; 1975 25(2):165–82. [PubMed: 1151432]
4. Barnett MH, Prineas JW. Relapsing and remitting multiple sclerosis: pathology of the newly forming lesion. Ann Neurol. Apr; 2004 55(4):458–68. [PubMed: 15048884]
5. Henderson AP, Barnett MH, Parratt JD, Prineas JW. Multiple sclerosis: distribution of inflammatory cells in newly forming lesions. Ann Neurol. Dec; 2009 66(6):739–53. [PubMed: 20035511]
6. Bruck W, Bitsch A, Kolenda H, Bruck Y, Stiefel M, Lassmann H. Inflammatory central nervous system demyelination: correlation of magnetic resonance imaging findings with lesion pathology. Ann Neurol. Nov; 1997 42(5):783–93. [PubMed: 9392578]
7. Grossman RI, Braffman BH, Brorson JR, Goldberg HI, Silberberg DH, Gonzalez-Scarano F. Multiple sclerosis: serial study of gadolinium-enhanced MR imaging. Radiology. Oct; 1988 169(1): 117–22. [PubMed: 3420246]
8. Lassmann H. The pathologic substrate of magnetic resonance alterations in multiple sclerosis. Neuroimaging Clin N Am. Nov; 2008 18(4):563–76. ix. [PubMed: 19068402]
9. Katz D, Taubenberger J, Raine C, Mcfarlin D, Mcfarland H. Gadolinium-Enhancing Lesions on Magnetic-Resonance-Imaging - Neuropathological Findings. Annals of Neurology. Aug.1990 28(2):243.
10. Alvarez JI, Cayrol R, Prat A. Disruption of central nervous system barriers in multiple sclerosis. Biochim Biophys Acta. Jul 7.2010
11. Mahad DJ, Lawry J, Howell SJL, Woodroofe MN. Longitudinal study of chemokine receptor expression on peripheral lymphocytes in multiple sclerosis: CXCR3 upregulation is associated with relapse. Multiple Sclerosis. Mar; 2003 9(2):189–98. [PubMed: 12708814]

12. Holman DW, Klein RS, Ransohoff RM. The blood-brain barrier, chemokines and multiple sclerosis. Biochim Biophys Acta. Feb; 2011 1812(2):220–30. [PubMed: 20692338]
13. Stolp HB, Dziegielewska KM. Review: Role of developmental inflammation and blood-brain barrier dysfunction in neurodevelopmental and neurodegenerative diseases. Neuropathol Appl Neurobiol. Apr; 2009 35(2):132–46. [PubMed: 19077110]
14. Capra R, Marciano N, Vignolo LA, Chiesa A, Gasparotti R. Gadolinium-pentetic acid magnetic resonance imaging in patients with relapsing remitting multiple sclerosis. Arch Neurol. Jul; 1992 49(7):687–9. [PubMed: 1497493]
15. Morgen K, Jeffries NO, Stone R, et al. Ring-enchancement in multiple sclerosis: marker of disease severity. Mult Scler. Jun; 2001 7(3):167–71. [PubMed: 11475440]
16. Davis M, Auh S, Riva M, et al. Ring and nodular multiple sclerosis lesions: a retrospective natural history study. Neurology. Mar 9; 2010 74(10):851–6. [PubMed: 20211910]
17. He J, Grossman RI, Ge Y, Mannon LJ. Enhancing patterns in multiple sclerosis: evolution and persistence. AJNR Am J Neuroradiol. Apr; 2001 22(4):664–9. [PubMed: 11290475]
18. Masdeu JC, Quinto C, Olivera C, Tenner M, Leslie D, Visintainer P. Open-ring imaging sign: highly specific for atypical brain demyelination. Neurology. Apr 11; 2000 54(7):1427–33. [PubMed: 10751251]
19. Bagheri MH, Meshksar A, Nabavizadeh SA, Borhani-Haghighi A, Ashjazadeh N, Nikseresht AR. Diagnostic value of contrast-enhanced fluid-attenuated inversion-recovery and delayed contrast-enhanced brain MRI in multiple sclerosis. Acad Radiol. Jan; 2008 15(1):15–23. [PubMed: 18078903]
20. Lovblad KO, Anzalone N, Dorfler A, et al. MR imaging in multiple sclerosis: review and recommendations for current practice. AJNR Am J Neuroradiol. Jun; 2010 31(6):983–9. [PubMed: 20019103]
21. Filippi M. Enhanced magnetic resonance imaging in multiple sclerosis. Mult Scler. Oct; 2000 6(5): 320–6. [PubMed: 11064441]
22. Nessler S, Boretius S, Stadelmann C, et al. Early MRI changes in a mouse model of multiple sclerosis are predictive of severe inflammatory tissue damage. Brain. Aug.2007 130:2186–98. [PubMed: 17617655]
23. Tofts PS, Kermode AG. Measurement of the Blood-Brain-Barrier Permeability and Leakage Space Using Dynamic Mr Imaging .1. Fundamental-Concepts. Magnetic Resonance in Medicine. Feb; 1991 17(2):357–67. [PubMed: 2062210]
24. Larsson HBW, Stubgaard M, Frederiksen JL, Jensen M, Henriksen O, Paulson OB. Quantitation of Blood-Brain-Barrier Defect by Magnetic-Resonance-Imaging and Gadolinium-Dtpa in Patients with Multiple-Sclerosis and Brain-Tumors. Magnetic Resonance in Medicine. Oct; 1990 16(1): 117–31. [PubMed: 2255233]
25. Kermode AG, Tofts PS, Thompson AJ, et al. Heterogeneity of blood-brain barrier changes in multiple sclerosis: an MRI study with gadolinium-DTPA enhancement. Neurology. Feb; 1990 40(2):229–35. [PubMed: 2300240]
26. Kurtzke JF. A new scale for evaluating disability in multiple sclerosis. Neurology. Aug; 1955 5(8): 580–3. [PubMed: 13244774]
27. Hawkins CP, Landon DN, Mackenzie F, Mcdonald WI, Munro PMG. Studies on the Mechanism of Blood-Brain-Barrier Breakdown in Chronic Relapsing Experimental Allergic Encephalomyelitis in the Guinea-Pig. Journal of Physiology-London. Jul.1990 426:P116. P.
28. McDonald WI, Miller DH, Barnes D. The pathological evolution of multiple sclerosis. Neuropathol Appl Neurobiol. Aug; 1992 18(4):319–34. [PubMed: 1528388]
29. Fazekas F, Soelberg-Sorensen P, Comi G, Filippi M. MRI to monitor treatment efficacy in multiple sclerosis. J Neuroimaging. Apr; 2007 17(Suppl 1):50S–5S. [PubMed: 17425736]
30. Daumer M, Neuhaus A, Morrissey S, Hintzen R, Ebers GC. MRI as an outcome in multiple sclerosis clinical trials. Neurology. Feb 24; 2009 72(8):705–11. [PubMed: 19073945]
31. Hochmeister S, Grundtner R, Bauer J, et al. Dysferlin is a new marker for leaky brain blood vessels in multiple sclerosis. J Neuropathol Exp Neurol. Sep; 2006 65(9):855–65. [PubMed: 16957579]

32. Wuerfel J, Bellmann-Strobl J, Brunecker P, et al. Changes in cerebral perfusion precede plaque formation in multiple sclerosis: a longitudinal perfusion MRI study. Brain. Jan; 2004 127(Pt 1): 111–9. [PubMed: 14570816]
33. Napoli I, Neumann H. Protective effects of microglia in multiple sclerosis. Exp Neurol. Sep; 2010 225(1):24–8. [PubMed: 19409897]
34. Barilaro A, Zellini F, Caleri F, et al. Kinetic of brain MRI gadolinium enhancing lesions in multiple sclerosis. European Journal of Neurology. Sep.2004 11:20.
35. van Horssen J, Brink BP, de Vries HE, van der Valk P, Bo L. The blood-brain barrier in cortical multiple sclerosis lesions. J Neuropathol Exp Neurol. Apr; 2007 66(4):321–8. [PubMed: 17413323]
36. Peterson JW, Bo L, Mork S, Chang A, Trapp BD. Transected neurites, apoptotic neurons, and reduced inflammation in cortical multiple sclerosis lesions. Ann Neurol. Sep; 2001 50(3):389–400. [PubMed: 11558796]
37. Werring DJ, Brassat D, Droogan AG, et al. The pathogenesis of lesions and normal-appearing white matter changes in multiple sclerosis: a serial diffusion MRI study. Brain. Aug; 2000 123(Pt 8):1667–76. [PubMed: 10908196]
38. Filippi M, Rocca MA, Martino G, Horsfield MA, Comi G. Magnetization transfer changes in the normal appearing white matter precede the appearance of enhancing lesions in patients with multiple sclerosis. Ann Neurol. Jun; 1998 43(6):809–14. [PubMed: 9629851]
39. Ludemann L, Warmuth C, Plotkin M, et al. Brain tumor perfusion: comparison of dynamic contrast enhanced magnetic resonance imaging using T1, T2, and T2* contrast, pulsed arterial spin labeling, and H2(15)O positron emission tomography. Eur J Radiol. Jun; 2009 70(3):465–74. [PubMed: 18359598]
40. Lacerda S, Law M. Magnetic resonance perfusion and permeability imaging in brain tumors. Neuroimaging Clin N Am. Nov; 2009 19(4):527–57. [PubMed: 19959004]

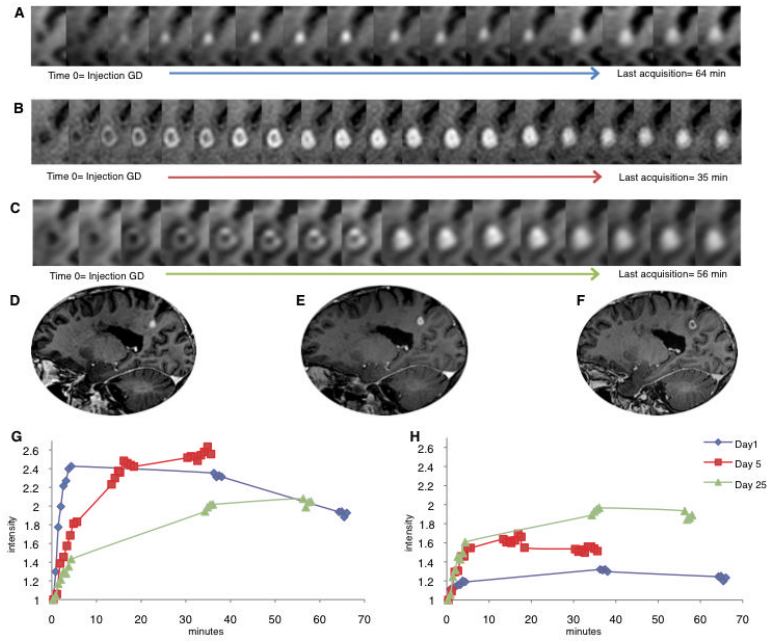

Figure 1.

Enhancement and expansion dynamics in a new lesion observed in a 40-year-old man with relapsing-remitting multiple sclerosis. On “Day 1” **(A)**, the scan on which the lesion was first observed, the enhancement pattern was centrifugal. By “Day 5” **(B)**, the enhancement pattern had become centripetal, and this pattern persisted on Day 25 **(C)**. Corresponding high-resolution T1-weighted scans are shown in **(D)** Day 1, 9.5 mm in diameter, 40 min after gadolinium injection; **(E)** Day 5, 11 mm in diameter, 6 min after gadolinium injection; and **(F)** Day 25, 12 mm in diameter, 6 min after gadolinium injection. The change in signal intensity over time, normalized to the pre-gadolinium scan, is shown for regions of interest in the center **(G)** and periphery **(H)** of the lesions. In the center, the slope and absolute values of enhancement intensity became progressively shallower as the lesion aged, whereas in the periphery the slope and the absolute values became progressively steeper.

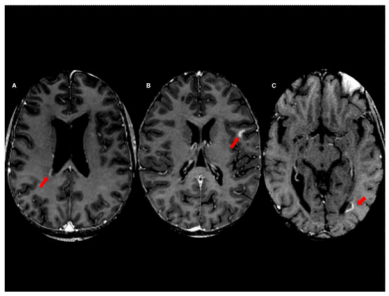

Figure 2.
Open ring-enhancing multiple sclerosis lesions (arrows) facing the lateral ventricles and cerebral cortex. **(A)** 40-year old man; **(B)** 30-year old woman; **(C)** 49-year-old man.

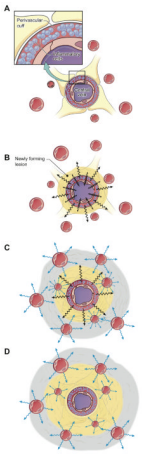

Figure 3.

Dynamics of blood-brain-barrier permeability in newly forming multiple-sclerosis lesions. **(A)** Perivascular cuff, the likely site of MS lesion initiation. **(B)** Opening of the central vein's blood-brain barrier, with outward spread of gadolinium (black bolts) resulting in the centrifugal enhancement. At this stage, peripheral vessels that are within and just beyond the border of the still expanding lesion are not yet open. **(C)** Secondary opening of the blood-brain barrier in peripheral vessels at the leading edge of the expanding lesion (blue bolts). Enhancement dynamics begin to change from centrifugal to centripetal. Gray shading represents the peripheral ring where centripetal enhancement begins. **(D)** Closing of the central vein, a relatively fast process (within 5 days in the lesion shown in Figure 1), which results in fully centripetal enhancement dynamics. As the lesion stops expanding and tissue repair begins, the blood-brain barrier closes even in peripheral vessels, and enhancement gradually ceases.

Table 1

Clinical characteristics

Group	Number	Sex	Age (years)	EDSS (range)	DD (years)	DMT
A	14 (18%)	57% F	37± 13	0-6	4 ± 4	35%
B	14 (18%)	64% F	41 ± 12	0-6	6 ± 6	50%
C	52 (65%)	60% F	43 ± 9	0-6.5	10 ± 7	73%

See Results for definition of the 3 groups. Abbreviations: RRMS=Relapsing remitting multiple sclerosis; DD=Disease Duration; EDSS=Expanded Disability Status Scale; F=Female; DMT=Disease-Modifying Treatment. Summary data are given as mean±standard deviation for age and SD and median (range) for EDSS.

Table 2

MRI parameters

	DCE (1.5T)	DCE (3.0T)	High-Res DCE	FSPGR-BRAVO	T1-weighted (1.5T)	FLAIR (3.0T)	FLAIR (1.5T)
FA	12 deg	15 deg	17 deg	13 deg	90 deg	90 deg	90 deg
TR	5.6 msec	5.6 msec	7.1 msec,	8.8 msec	600 msec	6000 msec	10 sec
TE	1.65 msec	1.84 msec	3.1 msec	3.84 msec	16 msec	12.7 msec	12.2 msec
VS	2×2×2 mm^3	2×2×2 mm^3	1×1×1 mm^3	1×1×1 mm^3	1×1×3 mm^3	1×1×1 mm^3	1×1×3 mm^3
TA	35 sec	35 sec	42 sec	4.2 min	3.9 min	8 min	4 min
TI				450 msec		1861 msec	2250 msec

Abbrevations: FA=flip angle; TR=repetition time; TE= echo time; VS=voxel size; TA=acquisition time; TI=inversion time; deg= degrees.

Table 3

Lesion enhancement pattern

Initial Pattern	N	Diameter (mm)	Dynamics		Final Pattern		
			Centripetal	Centrifugal	Nodular	Ring	Open-ring
Nodular	6	5.8 ± 1.2	0	100%	100%	0%	0%
Ring	22	9.6 ± 4.4	100%	0%	82%	18%	0%
Open-ring	6	12.8 ± 4.1	100%	0%	0%	0%	100%

Summary data are given as mean ± standard deviation. Abbreviations: N= number